Unimolecular decay paths of electronically excited species. V. The Ã2 B 1 state of H2CO+

C. Barbier, C. Galloy, and J. C. Lorquet

Citation: The Journal of Chemical Physics **81**, 2975 (1984); doi: 10.1063/1.448048
View online: http://dx.doi.org/10.1063/1.448048
View Table of Contents: http://scitation.aip.org/content/aip/journal/jcp/81/7?ver=pdfcov
Published by the AIP Publishing

Unimolecular decay paths of electronically excited species. V. The $\tilde{A}\,^2B_1$ state of H_2CO^+

C. Barbier[a], C. Galloy, and J. C. Lorquet[b]
Department de Chimie, Université de Liége, Sart-Tilman, B-4000 Liège, 1, Belgium

(Received 24 April 1984; accepted 22 May 1984)

The formaldehyde ion in its first excited state ($\tilde{A}\,^2B_1$) dissociates to $CO^+ + H_2$ by an electronically adiabatic mechanism. *Ab initio* calculations reveal, however, that the reaction path corresponds to a low energy trough around a conical intersection between the $\tilde{A}\,^2B_1/^2A'$ and $a\,^2A_1/^2A'$ states. This path is characterized by an energy barrier of 0.8 eV. The reaction mechanism is intrinsically multidimensional. Curvature of the reaction path brings about a strong coupling between the coordinate and the orthogonal degrees of freedom. For this reason, the final energy partitioning does not reflect the internal energy distribution at the top of the potential barrier. Energy is presumably released preferentially as translation and rotation. The criterion for reactivity is not purely energetic: the genuine bottleneck is not located at the top of the energy barrier but rather in the region where curvature of the reaction path is largest. The $\tilde{A}\,^2B_1$ state also dissociates to $HCO^+ + H$ fragments. A low-lying quartet state ($\tilde{a}\,^4B_2$) was studied but was found to play no role in the reaction. Direct coupling between state $\tilde{A}$ and the dissociation continuum of the ground state $\tilde{X}$ is suggested.

I. INTRODUCTION

There exists a substantial amount of information[1-5] about the dissociation of the formaldehyde positive ion H_2CO^+ and its deuterated isotopes D_2CO^+ and $HDCO^+$. In the Franck–Condon zone of the first excited state ($\tilde{A}\,^2B_1$) of the formaldehyde ion (which ranges from 14.1 to 15.5 eV, with energies measured from the lowest level of neutral H_2CO), two dissociation reactions have been observed:

$$H_2CO^+ (\tilde{A}\,^2B_1) \rightarrow HCO^+ (^1\Sigma^+) + H (^2S), \quad (1)$$

$$H_2CO^+ (\tilde{A}\,^2B_1) \rightarrow CO^+ (^2\Sigma^+) + H_2 (^1\Sigma_g^+). \quad (2)$$

These reactions were studied in detail by Guyon, Chupka, and Berkowitz (GCB)[1] by photoionization. From a mechanistic point of view, these experiments suffer from the disadvantage that they do not discriminate against autoionization. Since the latter process contributes largely to the fragmentation, the observed dissociation yields do not reflect exclusively the behavior of the electronic state of H_2CO^+. Autoionization is thus cluttering up the dynamics of unimolecular decomposition of polyatomic ions.

A theoretical study was then undertaken in this laboratory by Vaz Pires, Galloy and Lorquet (VPGL).[6] From *ab initio* calculations of potential energy surfaces, it was concluded that reactions (1) and (2) take place competitively after initial excitation to the first excited electronic state of H_2CO^+ ($\tilde{A}\,^2B_1$). This state is crossed by a dissociative $^2A_1$ state correlating with the $CO^+ + H_2$ asymptote. If the out-of-plane bending motion is taken into consideration, i.e., if the potential energy surfaces are studied in a multidimensional space, this genuine crossing is converted into a conical intersection. A circular, low-energy reaction path is then available which leads adiabatically to $CO^+ + H_2$ fragments. No energy barrier was detected by VPGL along this path.

In the mechanism suggested by these authors, this circular path is also involved in the production of the other kind of fragments (viz., $HCO^+ + H$), because it undergoes an additional crossing with the potential energy surface of the electronic ground state $\tilde{X}\,^2B_2$.

The model proposed by VPGL accounts for the photoionization experiments of GCB. A crossed beam study of the collisions between H_2^+ and CO provided additional support.[7]

Extensive investigation of reactions (1) and (2) was then carried out by Bombach, Dannacher, Stadelmann, and Vogt (BDSV).[2-4] In the so called photoelectron–photoion coincidence spectroscopy (PEPICS)[8] at fixed photon energy, the autoionization component is entirely suppressed. Using this technique, molecular ions can be prepared in specific vibronic states and their subsequent behavior can be studied as a function of their internal energy. The reaction products can be determined quantitatively and the partitioning of the available excess energy between internal and external degrees of freedom can be measured. The method was applied to the $\tilde{A}\,^2B_1$ state of H_2CO^+ and D_2CO^+. This demonstrated that a revision of the VPGL mechanism was necessary, at least at low energies. The reasons are as follows. Whereas the HCO^+ ions appear at an energy of 14.1 eV (corresponding to the vibrationless level of state $\tilde{A}\,^2B_1$ and to the thermochemical dissociation limit for CO^+ formation), the CO^+ ions are found to appear some 0.7 eV higher. The obvious explanation is that there exists a potential energy barrier of that magnitude along the reaction path, which was missed by VPGL because of excessive spacing between the points of the reaction path at which a geometry optimization was done. Moreover, this finding also makes necessary a reinvestiga-

[a] Present address: Facultés Universitaires, Départment de Physique, B-5000 Namur, Belgium.
[b] To whom correspondence should be addressed.

 0021-9606/84/192975-06$02.10

tion of the mechanism of production of HCO^+ ions, as will be seen later on.

Finally, there is an additional problem linked to the existence of metastable (i.e., long lived) parent ions. All the authors agree on the existence of a very slow dissociation process in the case of the perdeuterated species:

$$D_2CO^+ \rightarrow DCO^+ + D, \quad (3)$$

and they all agree about its average lifetime being longer than $10\,\mu s$ (detailed values have been given by BDSV[2]). The existence of a corresponding process in the nondeuterated species is denied by GCB and by BDSV. However, Wankenne *et al.*[5] have observed it in all three species H_2CO^+, D_2CO^+, and $HDCO^+$ and have described strong and puzzling isotope effects. The mechanism is then dominated by autoionization.

All this makes necessary a reinvestigation of the potential energy surfaces of the formaldehyde ion, especially that of state $\tilde{A}\,^2B_1$. The results of this study are presented in Sec. II. It will emerge that there is indeed a barrier along the path and thus that the VPGL mechanism becomes invalid at low energies. This requires a reinterpretation of the mechanism of production of HCO^+ fragments which is reinvestigated in Sec. III.

II. PRODUCTION OF CO^+ IONS

A. Method of calculation

The potential energy surfaces were calculated by the standard LCAO-MO-SCF-CI method using the MOLALCH system of programs.[9] The atomic basis set for C and O atoms is the standard Huzinaga $9s\ 5p$ Cartesian Gaussian basis set[10] with Dunning's $3s\ 2p$ contractions.[11] For H atoms, the $[4s/2s]$ set was used with a scaling factor of 1.2. The calculations were done in the C_s point group. The CI matrix of the $\tilde{A}\,^2B_1/^2\tilde{A}'$ state included all of the monoexcitations and part of the diexcitations from six reference configurations listed in Table I. The matrix included 771 configuration state functions. (CSF's).

The MO's used in the CI calculation were obtained from a SCF calculation on an intermediate configuration of the neutral molecule, viz.....$(6a')^1\ (7a')^1\ (2a'')^2$. When MO's become degenerate this provides a homogeneous level of approximation.[12] In two particular cases (viz., for two slightly pyramidal conformations) no closed-shell or open-shell SCF procedure was able to converge in spite of numerous attempts. In such a pathological situation, the SCF step was suppressed, and the CI matrix was built on the natural orbitals (NO's) obtained at the corresponding planar geometry. In order to make certain that this *ad hoc* procedure did not introduce a bias in the wave function, a second CI calculation was carried out starting with the natural orbitals produced by a first calculation.

TABLE I. Reference electronic configurations used in the CI calculation of the $\tilde{A}\,^2B_1/^2A'$ state.

ϕ_1	$(1a')^2...(5a')^2(1a'')^2(6a')^1(2a'')^2$
ϕ_2	$(1a')^2...(5a')^2(1a'')^2(6a')^2(7a')^1$
ϕ_3	$(1a')^2...(5a')^2(1a'')^2(6a')^2(8a')^1$
ϕ_4	$(1a')^2...(5a')^2(1a'')^2(6a')^1(7a')^2$
ϕ_5	$(1a')^2...(5a')^2(1a'')^1(6a')^2(7a')^1(2a'')^1$
ϕ_6	$(1a')^2...(5a')^2(1a'')^2(6a')^1(7a')^1(8a')^1$

B. The energy barrier

The reaction path was determined by optimizing the nuclear geometries at seven particular points along the reaction coordinate. The results are given in Table II and in Fig. 1. The $\tilde{A}\,^2B_1/^2A'$ state was found to be slightly nonplanar in its equilibrium geometry. This is confirmed by spectroscopic observations on the Rydberg states converging toward this state.[1]

According to our calculations, there is an energy barrier (measured from the bottom of the potential energy surface of state $\tilde{A}$ to the top of the barrier) equal to 0.82 eV. The barrier to the reverse reaction (i.e., measured from $CO^+ + X_2$) is equal to 0.76 eV. The latter estimate is in nice agreement with BDSV's measurements [0.72 ± 0.1) eV and (0.79 ± 0.1) eV for H_2CO^+ and D_2CO^+, respectively].

C. The reaction path

In order to facilitate the discussion, the reaction path will be partitioned into several sections (cf. Figs. 1 and 2 and Table II).

(i) The first part (I) corresponds to the energy increase from the bottom of state $\tilde{A}$ to the top of the energy barrier. The CH bond distance increases from 1.09 to 1.25 Å, whereas the other geometrical parameters (R_{CO}, HĈH, θ) undergo very little change. This part correspond to the quadratic force field associated with the stable H_2CO^+ ion in its electronic configuration Φ_1. R_{CH} is then a very good parameter for the description of the reaction coordinate.

(ii) Part II involves an insignificant change of the R_{CH} bond distance, viz. from 1.25 to 1.26 Å (i.e., immediately after the top of the potential energy barrier which is at 1.25 Å). Within this narrow range, the other geometrical param-

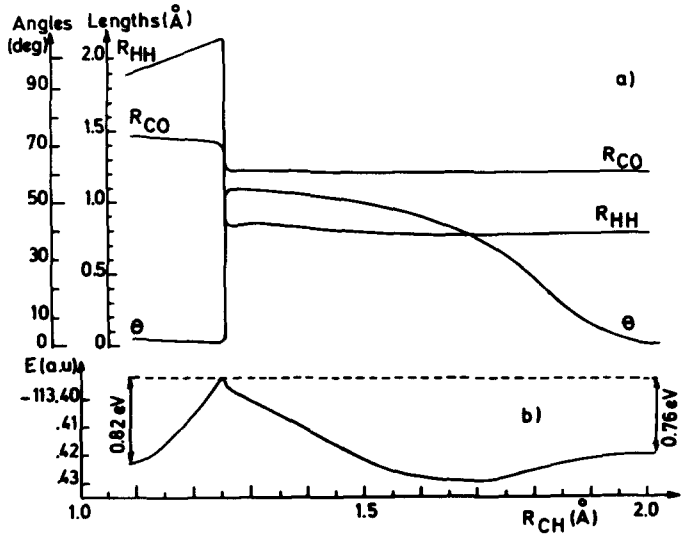

FIG. 1. (a) Variation of the geometrical parameters of the H_2CO^+ ion along the reaction path leading to $CO^+ + H_2$ fragments. (b) Cross section in the potential energy of surface of state $\tilde{A}$ along the same path. The reaction coordinate is specified by the value of its component of the CH bond distance.

TABLE II. Geometrical optimization of the reaction path associated with the production of $CO^+ + H_2$ fragments.

R_{CH}(Å)	R_{CO}(Å)	θ(°)	$\widehat{HCH}$(°)	R_{HH}(Å)	$E_{A^2A'}$(a.u.)	$E_{^2A'(2)}$(a.u.)	Leading Config.
1.09	1.46	2.6	121.6	1.9	− 113.423 06	− 113.348 61	ϕ_1
1.25	1.42	1.6	119.3	2.16	− 113.392 67	− 113.348 17	ϕ_1
1.26	1.23	54.6	38.4	0.83	− 113.396 41	− 113.192 22	ϕ_2
1.3	1.23	53.9	38.8	0.86	− 113.400 54	− 113.195 65	ϕ_2
1.54	1.20	48.0	29.5	0.78	− 113.426 02	− 113.223 83	ϕ_2
1.7	1.19	36.6	26.0	0.76	− 113.430 34	− 113.234 22	ϕ_2
2.0	1.19	0.0	22.5	0.78	− 113.420 65	− 113.229 48	ϕ_3

eters undergo dramatic modifications. The ion becomes suddenly strongly pyramidal, whereas the CO and HH bond distances relax and adopt their equilibrium distances in the CO^+ and H_2 fragments. Thus, the first task of the molecular ion as it begins to leave the potential energy maximum is to "prepare" the future fragments at their equilibrium geometry. This involve virtually no separation in space, but rather a very sudden change in the electronic configuration. The leading term of the CI expansion is ϕ_1 at $R_{CH} = 1.25$ Å and ϕ_2 at 1.26 Å.

In other words, the reaction path has a negligible component on the R_{CH} bond distance in this range. The apparently unrealistic, much too abrupt variations of θ, R_{HH} and R_{CO} between $R_{CH} = 1.25$ and 1.26 Å are a consequence of the inappropriate nature of the R_{CH} coordinate for the description of the reaction path in this particular range.

(iii) Part III extends from $R_{CH} = 1.26$ to 2.0 Å. The R_{CO} and R_{HH} distances change very little. The reaction path has again its major component on the CH bond distance, but a relaxation of the angle of pyramidalization from a highly bent to the planar geometry also takes place. Thus, part III of the reaction path corresponds to the repulsion between a CO^+ ion and a hydrogen molecule in a global electronic state described by configuration Φ_2.

(iv) Part IV extends from $R_{CH} = 2.0$ Å onwards. The ion is again planar and the leading electronic configuration is Φ_3.

Since energy partitioning between translation, rotation, and vibration of fragments is determined by the characteristics of that part of the reaction path which extends from the transition state to the fragments onward, it was decided to take a closer look at it. As a symmetry plane is preserved everywhere along the reaction path (A' representation of point group C_s), only four coordinates are necessary.

A system of internal coordinates consisting of three bond lengths (R_{CH}, R_{CO}, R_{HH}) plus the pyramidalization angle θ was adopted. In connection with previous work on the differential geometry of chemically reacting systems,[13] it is important to note that the description of a reaction path in terms of internal coordinates presents a twofold complication. First, internal coordinates are general curvilinear, non-Cartesian coordinates. Moreover, they span a configuration space which may be non-Euclidean, i.e., intrinsically curved. This has been found to be the case in the present study, but the results will not be reported here.[14] Suffice it to say that the curvilinear nature of the corrdinates R_{CH}, R_{CO}, θ, and R_{HH}, and the non-Euclidean metric of the four-dimensional configuration space have been carefully taken into account in the geometrical study of the reaction path.

A curvilinear abscissa s was calculated along the reaction path with the origin taken at the top of the energy barrier ($R_{CH} = 1.25$Å). The function s (R_{CH}) is represented in Fig. 2. The use of such a curvilinear abscissa is much more appropriate for a study of the geometrical readjustments along the reaction path (Figs. 3 and 4). When calculated as a

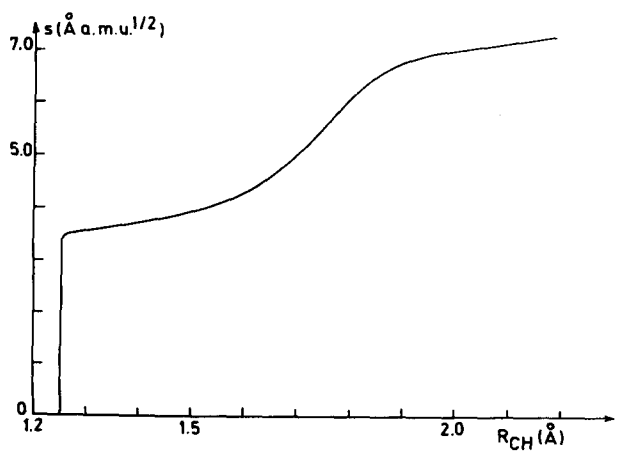

FIG. 2. Variation of the curvilinear abscissa s along the reaction path as a function of R_{CH}.

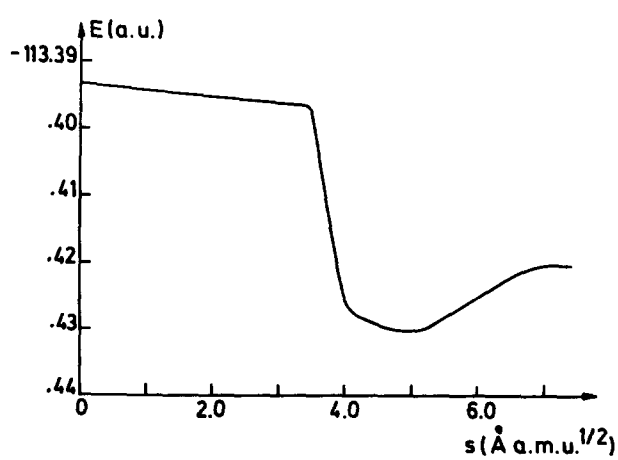

FIG. 3. Potential energy of state $\tilde{A}$ along the reaction path as a function of the curvilinear abscissa s.

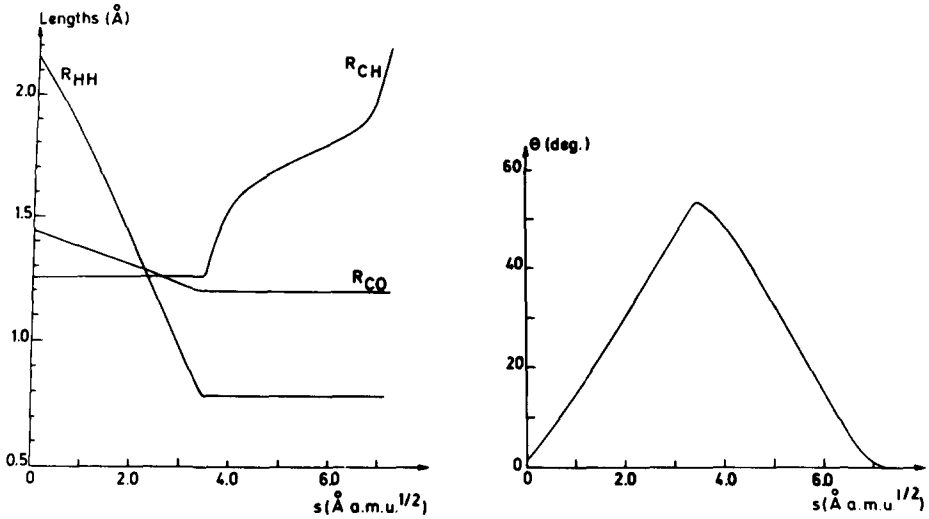

FIG. 4. Variation of the geometrical parameters as a function of the curvilinear abscissa s along the reaction path.

function of s, the curvature of the reaction path is found to be small everywhere except at two places: At the junction of regions II and III (around $R_{CH} \simeq 1.259$ Å) on the one hand, and at the junction of regions III and IV (around $R_{CH} \cong 1.97$ Å) on the other hand. This confirms the fact that at these junctions, the reaction path undergoes an important reorientation.

The components of the unitary tangent to the reaction path have also been calculated.[14] They confirm the previous analysis.

D. Energy partitioning

An important consequence is that a strong "bobsled effect"[15] has to be expected at these regions of high curvature. This consists in a strong coupling between the radial motion along the reaction path and the orthogonal degrees of freedom. This phenomenon is also named "exit-channel interaction." It takes place as the fragments separate in space and has important consequences on energy partitioning into the translational, rotational, and vibrational degrees of freedom,[16] as will be seen presently.

Let us consider the limit case in which the internal energy of the ion is just sufficient to overcome the potential barrier. If no curvature were present in the reaction path, one would expect a final energy distribution with all the reverse activation energy appearing as translational energy. The presence of zones of high curvature modifies this expectation by allowing energy transfer from the reaction coordinate to perpendicular degrees of freedom. As the system enters the first region of high curvature (which extends between $R_{CH} = 1.256$ and 1.265 Å), it has accumulated about 0.1 eV in the reaction coordinate, and it is not unreasonable to consider the limit case in which this entire amount of energy is transferred to the orthogonal modes. Between 1.265 and 1.95 Å, the reaction path has virtually no curvature and the corresponding energy release (0.66 eV) goes probably entirely into the reaction coordinate. A second region of high curvature is encountered between 1.95 and 2.05 Å, and here again some of the latter energy release will be transferred to internal coordinates. The final balance cannot be estimated by qualitative arguments, but it is not unreasonable to expect roughly equal shares between translational and internal energy releases. BDSV observe[3] that about 60% of the available energy appears as fragment translation. How much of the rest goes into vibration and how much into rotation? The first energy release of 0.1 eV as R_{CH} varies from 1.25 to 1.26 Å has to flow into the three main components of the reaction path in Region II, i.e., R_{CO}, R_{HH}, and θ. An amount of 0.1 eV cannot induce vibrational excitation of H_2 or CO^+, even by a single quantum. In the subsequent part of the reaction path (from $R_{CH} = 1.26$ to 2.0 Å), the reaction path has major components on R_{CH} and θ, not on R_{CO} and R_{HH}. Therefore, little energy flow into the latter degrees of freedom is expected. This leads us to the conjecture that the final energy partitioning should be dominated by translation and by rotation.

E. Rate constants

A few trajectory calculations have been carried out in order to compare the roles played by the energy barrier and by the region of high curvature in the requirements to be fulfilled by a nuclear trajectory to contribute to reactivity. Pechukas[17] has discussed the reasons why, as a consequence of the multidimensional nature of the reaction path, the best location of the classical transition state is not necessarily at the top of a potential energy barrier. The potential energy was written in the form

$$V(R_{CH}, R_{CO}, R_{HH}, \theta) = V_0(R_{CH}) + \sum_{j=1}^{3} \frac{1}{2} k_j(R_j)[R_j - R_j^{eq}(R_{CH})]^2, \quad (4)$$

where $V_0(R_{CH})$ is the potential energy along the reaction path resulting from *ab initio* calculations. (Fig. 1) and the quantities indexed by a subscript j refer to the other three degrees of freedom. The force constants of the latter were allowed to vary along the reaction path and were obtained by a Lagrange quadratic interpolation. The origin of all the trajectories was taken at the top of the potential energy barrier. The initial conditions were such that the trajectories were heading toward the products with a total energy of about 0.2 eV above the top of the barrier. A total number of 33 trajectories were calculated by an Adams–Moulton–Bashforth routine[18] with an integration step of 0.1 a.u. None was found to reach the dissociation asymptote. Most of them were driven back in a very short time and none was able to cross the

region where the curvature of the reaction path is very large.

This behavior is at odds with the conventional textbook picture. The present case of chemical reactivity cannot be studied as a one-dimensional motion along a reaction path completely decoupled from the other modes. As discussed by Pechukas,[17] a purely energetic criterion is only valid for a one-dimensional problem. In the present reaction, the genuine bottleneck is associated with a region of high curvature which results from the multidimensional character of the reaction path. This region acts as a filter which rejects many trajectories having enough energy to reach the asymptote.

It is interesting to recall here Wigner's criterion[19] according which transition state theory is exact only if there exists a dividing surface across the reaction path which is never crossed twice by any classical trajectory. The present calculations show clearly that this criterion is not at all fulfilled by a dividing surface located at the top of the energy barrier. Only the variational version of transition state theory[20] might be expected to lead to satisfactory results. Presumably, this procedure would locate the dividing surface deep in region II.

We note finally that there would be little point in pursuing further the analysis of the problem by classical trajectories, because in a reaction controlled by a region where the reaction path has a strong curvature, the reactive flux is dominated by tunneling effects known as "corner-cutting".[21] A study of these effects requires quantum corrections.

III. PRODUCTION OF HCO^+ IONS

A. The surface crossing between states $\tilde{A}$ and $\tilde{X}$

The mechanism proposed by VPGL to account for the production of HCO^+ fragments from the first excited state $\tilde{A}\,^2B_1$ consists in a radiationless transition whereby the population of state $\tilde{A}$ (whose zero-point energy is at 14.1 eV) is converted to state $\tilde{X}$ (whose dissociation asymptote is at 11.9 eV). A crossing between these two states exists. The low-energy circular trough which leads to the $CO^+ + H_2$ fragments is crossed by the potential energy surface of ground state $\tilde{X}\,^2B_2/^2A''$. Since no barrier was detected by VPGL along that path, they predicted that even the vibrationless level of state $\tilde{A}$ could decay to $HCO^+ + H$ fragments via this mechanism. However, more accurate calculations were carried out in the present study. They revealed that the crossing between states $\tilde{A}$ and $\tilde{X}$ takes place approximately at R_{CH} 1.3 Å, i.e., slightly after the top of the energy barrier, at an energy of about 14.8 eV.

Therefore, at least two mechanisms seem to be involved in the interal conversion from state $\tilde{A}$ to state $\tilde{X}$ and hence in the production of the HCO^+ ions. The mechanism suggested by VPGL seems to be valid for the vibrational levels whose energy is higher than 14.8 eV (14.9 eV for the deuterated compound). This process is expected to be characterized by a relatively high rate constant. However, it cannot take place for the low-lying vibrational levels, i.e., for the first six vibrational levels whose lifetime has been measured[2] by BDSV in the case of D_2CO^+. These levels are found to dissociate with a remarkably low rate constant. Thus, another mechanism must be looked for to account for the slow radiationless transition undergone by these levels. One possibility is examined in the following paragraph.

B. The low-lying quartet state

A transfer of population between states $\tilde{A}$ and $\tilde{X}$ might be due to the existence of a low-energy state which would act as an intermediate. The most likely candidate for this is a $^4B_2$ state corresponding to the $(5a_1)^2(1b_2)^2(1b_1)^1(2b_2)^1(2b_1)^1$ configuration. The mechanism of production of HCO^+ ions at low energies would then be represented by the scheme

$$\tilde{A}\,^2B_1 \rightarrow \tilde{a}\,^4B_2 \rightarrow \tilde{X}\,^2B_2 \rightarrow HCO^+ + H. \quad (5)$$

Such a process consists of a double spin-forbidden intersystem crossing involving probably tunneling at least at threshold. This would be consistent with the very low value of the rate constant which characterizes the dissociation of at least the perdeuterated compound. Unfortunately, this mechanism had to be discarded for the following reasons.

(i) Elementary considerations about the bonding and antibonding nature of the relevant MO's suggest that the CO bond distance should increase along the sequence $\tilde{X}\,^2B_2$, $\tilde{A}\,^2B_1$, $\tilde{a}\,^4B_2$, and this is borne out by actual calculations. The CO bond distance might thus be the reaction coordinate for the intersystem crossings of Eq. (5). However, a cross section in the potential energy surfaces of both states along the CO bond distance with the other geometrical parameters frozen at a value close to the equilibrium geometry of state $\tilde{A}$ was done with a split-shell basis set of AO's (the Huzinaga–Dunning [9s 5p/3s 2p] for C and O and [4s/2s] for H basis set)[10–11] and a medium size for the CI matrices (473 and 856 CDF's for $\tilde{A}\,^2B_1$ and $\tilde{a}\,^4B_1$, respectively). The MO's were obtained from a SCF calculation on an intermediate triplet state with a ... $(1b_2)^2(1b_1)^2(2b_2)^1(2b_1)^1$ configuration. This revealed no crossing and hence no possibility for a transfer of population.

(ii) The most important piece of information in the assessment of the validity of the mechanism described by Eq. (4) is obviously the energy difference ΔE between states $\tilde{A}$ and $\tilde{a}$ at their equilibrium geometry. One can not account for the depletion of the vibrationless level of state $\tilde{A}$ by mechnaism (4) unless ΔE is very small, i.e., equal to zero, or, still better, negative. In order to get rid of any bias in the calculation of this quantity, various calculations were carried out. They differed by the size of the AO basis set (decontraction of the Gaussians, inclusion of Rydberg AO'S and of $3d_c$, $3d_0$, and $2p_H$ polarization functions), the nature of the SCF orbitals (use of closed- or open-shell MO's), and the size of the CI expansion. Seven different pairs of calculations, of increasing accuracy were carried out. In addition, the stability of the results was checked by repeating the CI calculations in terms of the NO's found from a first calculation. It is not essential to report all of these calculations in detail. Optimization of the nuclear geometry of states $\tilde{A}$ and $\tilde{a}$ led to values reported in Table III. Values of ΔE ranging between 0.7 and 1.5 eV were obtained. Our best values resulted from a double-zeta + polarization basis set (the Huzinaga–Dunning[10–11] [9s 5p/4s 2p] GTO + 3d AO's (with $\alpha = 1.0$)[22] on carbon and oxygen and [4s/2s] GTO + 2p AO's (with $\alpha = 0.8$)[22] on the hydrogens). Open-shell MO's were calculated independently for each ionic state. The CI expansion

TABLE III. Optimized geometries of states $\tilde{A}\,^2B_1/^2A'$ and $\tilde{a}\,^4B_2/^4A''$. Distances in angström units and angles in degrees.

State	R_{CH}	R_{CO}	R_{HH}	HCH	θ
$\tilde{A}$	1.10	1.49	1.91	120	2.6
$\tilde{a}$	1.09	1.61	2.0	134	50

included 1333 CSF's for $\tilde{A}\,^2B_1$ and 2418 CSF's for a $\tilde{a}\,^4B_2$. In C_{2v} geometry, the absolute energies were -113.5347 a.u. for $\tilde{A}\,^2B_1$ and -113.4952 a.u. for $\tilde{a}\,^4B_2$. Out-of-plane bending of the molecular ion led to a further slight stabilization of both states (0.17 eV for state $\tilde{a}$, and 0.19 eV for state $\tilde{A}$). This gave rise to a value of ΔE equal to 1.07 and 1.09 eV for the planar and bent geometries, respectively. In conclusion, the mechanism represented by Eq. (4) has to be discarded as well.

IV. CONCLUSIONS

Concerning the mechanism of production of CO^+ ions, the *ab initio* calculations confirm the existence of a highly specific reaction path and establish the existence of an energy barrier along this path. Quantitative agreement with the experimental value of the AE of the CO^+ ions has been obtained. As a result of the peculiar shape of the reaction path, we suggest that the excess energy is released preferentially on the translational and rotational degrees of freedom with exclusion of vibration. This reaction provides an example where the transition state is not associated with an energy barrier, but with a region of high curvature of the reaction path.

Concerning the production of HCO^+ fragments, neither the mechanism proposed by VPGL, nor mechanism (4) can account for the predissociation of low-energy levels. The former may play a role at energies higher than 0.8 eV, i.e., at the end of the Franck–Condon zone (in a direct excitation process) or for those ions which cascade down from upper states. The mechanism represented by Eq. (4) is probably too slow to compete with any other one.

The only mechanism we can suggest for this reaction is a direct interaction with the continuum of the ground state. This has been suggested both for diatomic[23] and for large polyatomic molecules,[24] and it would be interesting to see how important such a mechanism would be in the case of a small polyatomic system. The vibrational overlap associated with such a process is very small and would bring about a low rate constant which would account for the experimental results. It remains to be seen whether quantitative agreement would be obtained with the distribution of lifetimes measured by BDSV as a function of the vibrational quantum number, and for the various isotope effects experimentally detected. This is left for a further study.

ACKNOWLEDGMENTS

The authors are grateful to Dr. J. Dannacher, Professor J. Momigny, Dr. J. P. Stadelmann, and Dr. H. Wankenne for private communications and discussions of the experimental aspects of the problem. They are indebted to Dr. D. Dehareng for her help in the trajectory calculations. This work has been supported by research grants from the Fonds de la Recherche Fondamentale Collective and from the Belgian Government (Action de Recherche Concertée).

[1] P. M. Guyon, W. A. Chupka, and J. Berkowitz, J. Chem. Phys. **64**, 1419 (1976).
[2] R. Bombach, J. Dannacher, J. P. Stadelmann, and J. Vogt, Chem. Phys. Lett. **76**, 429 (1980).
[3] R. Bombach, J. Dannacher, J. P. Stadelmann, and J. Vogt, Chem. Phys. Lett. **77**, 399 (1981).
[4] R. Bombach, J. Dannacher, J. P. Stadelmann, and J. Vogt, Int. J. Mass Spectrom. Ion Phys. **40**, 275 (1981).
[5] H. Wankenne, G. Caprace, and J. Momigny, Int. J. Mass Spectrom. Ion Process. **57**, 149 (1984).
[6] M. Vaz Pires, C. Galloy, and J. C. Lorquet, J. Chem. Phys. **69**, 3242 (1978).
[7] R. M. Bilotta, F. N. Preuninger,and J. M. Farrar, J. Chem. Phys. **72**, 1583 (1980).
[8] J. Dannacher, and J. Vogt, Helv. Chim. Acta **61**, 361 (1978).
[9] The joint MOLECULE/ALCHEMY system incorporates the MOLECULE integral program and the ALCHEMY SCF, MCSCF, and CI programs. MOLECULE was written by J. Almlöf and the ALCHEMY programs were developed at the IBM San Jose Research Laboratories. The principal authors of ALCHEMY were P. S. Bagus, B. Liu, A. D. McLean, and M. Yoshimine.
[10] S. Huzinaga J. Chem. Phys. **42**, 1293 (1965).
[11] T. H. Dunning, J. Chem. Phys. **53**, 2823 (1970).
[12] R. McWeeny, Mol. Phys. **28**, 1273 (1974); L. Salem., C. Leforestier, G. Segal, and R. Wetmore, J. Am. Chem. Soc. **97**, 479 (1975); J. Liévin and G. Verhaegen, Theor. Chim. Acta **42**, 42 (1976).
[13] A. Tachibana and K. Fukui, Theor. Chim. Acta **49**, 321 (1978); X. Chapuisat, A. Nauts, and G. Durand, Chem. Phys. **56**, 91 (1981); A. Nauts and X. Chapuisat, Chem. Phys. Lett. **85**, 212 (1982); Chem. Phys. **76**, 349 (1983).
[14] C. Barbier (to be published).
[15] R. A. Marcus, J. Chem. Phys. **45**, 4493, 4500 (1966); W. H. Miller, N. C. Handy, and J. E. Adams, J. Chem. Phys. **72**, 99 (1980).
[16] R. A. Marcus, Faraday Discuss. Chem. Soc. **55**, 379, 381 (1973). S. Kato and K. Morokuma, J. Chem. Phys. **73**, 3900 (1980).
[17] P. Pechukas, in *Dynamics of Molecular Collisions*, edited by W. H. Miller (Plenum, New York, 1976), Part B, p. 269.
[18] C. W. Gear, *Numerical Initial Value Problems in Ordinary Differential Equations* (Prentice Hall, New York, 1971).
[19] E. Wigner, Trans. Faraday Soc. **34**, 29 (1938).
[20] B. C. Garrett and D. G. Truhlar, J. Chem. Phys. **70**, 1593 (1979); D. G. Truhlar and B. C. Garrett, Acc. Chem. Res. **13**, 440 (1980); D. G. Truhlar, W. L. Hase, and J. T. Hynes, J. Phys. Chem. **87**, 2664 (1983); W. L. Hase, Acc. Chem. Res. **16**, 258 (1983).
[21] R. A. Marcus and M. E. Coltrin, J. Chem. Phys. **67**, 2609 (1977); B. C. Garrett and D. G. Truhlar, J. Phys. Chem. **83**, 200 (1979); **83**, 1079 (1979); B. C. Garrett, D. G. Truhlar, A. F. Wagner, and T. H. Dunning, J. Chem. Phys. **78**, 4400 (1983); D. K. Bond, J. N. L. Connor, B. C. Garrett, and D. G. Truhlar, **78**, 5981 (1983).
[22] H. F. Schaefer III, *The Electronic Structure of Atoms and Molecules: A Survey of Rigorous Quantum Mechanical Results* (Addison–Wesley, London, 1972), p. 78.
[23] S. Durmaz and J. N. Murrell, Trans. Faraday Soc. **67**, 3396 (1971); J. Tellinghuisen and D. L. Albritton, Chem. Phys. Lett. **31**, 91 (1975); A. L. Roche and J. Tellinghuisen, Mol. Phys. **38**, 129 (1979).
[24] W. Siebrand, in *Dynamics of Molecular Collisions*, edited by W. H. Miller (Plenum, New York, 1976), Part A, p. 249.